Real-Time 1−2 Plane SAXS Measurements of Molecular Orientation in Sheared Liquid Crystalline Polymers

Franklin E. Caputo and Wesley R. Burghardt*

Department of Chemical Engineering, Northwestern University, Evanston, Illinois 60208

Received May 2, 2001; Revised Manuscript Received July 15, 2001

ABSTRACT: We report studies on the average molecular orientation state in steady and transient shear flow of two lyotropic liquid crystalline polymers: poly(benzyl glutamate) [PBG] and hydroxypropylcellulose [HPC], both in *m*-cresol solution. An annular cone and plate X-ray shear cell is used to probe molecular orientation in the "1−2" plane, allowing simultaneous measurements of the degree of anisotropy and the average orientation angle relative to the flow direction. In steady shear flow, molecular orientation increases with shear rate in both materials. Comparisons with separate measurements in the "1−3" plane indicate that both materials exhibit a macroscopically biaxial orientation distribution function. The orientation angle is always small and exhibits a sign change from positive to negative values with increasing shear rate. In transient flows, anisotropy and orientation angle both exhibit damped oscillations that scale with shear strain. The Larson−Doi polydomain model is in qualitative agreement with data collected on PBG in flow reversal, but only after an initial transient response seen in the experiments over the first several strain units following the reversal. Following step-increase and step-decrease of shear rate, the Larson−Doi model makes qualitatively correct predictions of anisotropy but qualitatively incorrect predictions of the transient average orientation angle.

Introduction

In situ measurements of flow-induced structural changes can provide crucial insights into the rheology and dynamics of complex fluids.[1,2] This has certainly been true in the case of liquid crystalline polymers (LCPs), which can respond to shear at multiple structural levels. Lyotropic LCPs are known to exhibit director tumbling in shear flow at low rates: hydrodynamic torques on the nematic director, **n**, tend to rotate it in shear flow.[3,4] Tumbling is associated with many of the unusual rheological phenomena that have been reported in lyotropes.[2] Rather than promoting macroscopic alignment, tumbling in shear flow acts to disrupt alignment and generates orientational defects that lead to a *polydomain texture*, in which the director field is an extraordinarily complex function of position. As a result, rheological and structural measurements on sheared LCPs not only sample the response of the locally anisotropic molecular orientation state but also average over the distribution of director orientation present in these textured fluids.[5]

We have reported extensive studies of molecular orientation in both lyotropic and thermotropic liquid crystalline polymers, using optical birefringence and X-ray scattering methods to measure the average molecular orientation state.[5−12] While these previous studies have elucidated the microstructural origins of complex rheological behavior in LCPs, in most cases they have provided only incomplete information about the average molecular orientation state. This is because most of these studies have used a rotating parallel disk shear flow geometry, in which the incident light or X-ray beam passes along the local velocity gradient direction. Structural anisotropy in the test fluid is then probed in the so-called "1−3" plane ("1" denotes shear flow direction, "2" denotes velocity gradient direction, "3" denotes the neutral or vorticity direction). An exception to this has been use of an angled light flow birefringence technique by Hongladarom and co-workers to study *steady* flows of lyotropic LCPs.[8,10] This method proved to be very sensitive, accurately measuring small average orientation angles away from the flow direction in LCPs. It also provided estimates of the degree to which the average 3-D orientation state in sheared LCPs is uniaxial. (Despite the fact that nematic LCPs exhibit a uniaxially symmetric molecular orientation distribution at equilibrium, there is no reason to expect that the average orientation state under shear should be uniaxial. In textured polydomain LCPs at low shear rates, the distribution of director orientation need not be uniaxial even though the local molecular orientation state should remain uniaxial at low Deborah number. At high shear rates, nonlinear viscoelastic effects can also break the uniaxial symmetry at the molecular level.)

The angled birefringence method employed by Hongladarom and co-workers is laborious and poorly suited for tracking rapid orientation changes in transient flows. This is unfortunate, since transient experiments in the 1−3 plane have revealed some limitations in the ability of the Larson−Doi polydomain model[13] to correctly predict the transient orientation dynamics of LCPs in time-dependent flows such as step changes in shear flow rate and direction. Moreover, birefringence provides a rather limited characterization of the orientation state of complex fluids relative to scattering methods[11,12] and is limited to materials that are transparent. Here we present data collected using an X-ray shear cell that allows anisotropy to be probed in the 1−2 plane. Together with synchrotron radiation and fast 2-D detectors, this enables transient measurements of both the degree and direction of molecular orientation within the 1−2 plane. These methods are applied to study steady and transient molecular orientation in two lyotropic LCP solutions: 13.5 wt % poly(benzyl glutamate) (PBG)

* Corresponding author: e-mail w-burghardt@northwestern.edu; tel (847) 467-1401; fax (847) 491-3728.

10.1021/ma0107556 CCC: $20.00
Published on Web 08/17/2001

in *m*-cresol and 27 wt % hydroxypropylcellulose (HPC) in *m*-cresol. We use these data to conduct deeper tests of the Larson−Doi polydomain model's orientation predictions than have been possible to date. Prior to a description of the experimental methods and results, we review this model and its transient orientation predictions for flows of interest.

Transient Orientation Predictions: Larson−Doi Model

The Larson−Doi model treats the structure and rheology of textured liquid crystalline polymers by averaging the fluid's response over a distribution of domain orientations within the polydomain sample. This averaging is performed on a volume of fluid that is large compared to the characteristic domain size (typically on the order of microns) but small compared to the macroscopic flow dimensions. The model is built upon the linear continuum theory of liquid crystal hydrodynamics (Leslie−Ericksen theory[14]) and hence is restricted to low shear rates where flow does not significantly perturb the local distribution of molecular orientation around the director. The parameters that appear in the continuum theory (i.e., Leslie coefficients) are predicted using the Doi molecular theory for lyotropic solutions of rodlike polymers.[15,16] As a result, the Larson−Doi model accounts for director tumbling, as predicted by the Doi theory at low rates.[17] The model also accounts, in a phenomenological way, for the distortional elasticity—present in all nematics—that opposes spatial variations in the director field.

The Larson−Doi model consists of evolution equations for the mesoscopically averaged fluid structure and a constitutive equation for the average stress. The model is known to make good qualitative predictions of certain rheological behavior seen in lyotropes at low rates,[13] namely the presence of damped oscillatory stresses in response to transient changes in shear rate or direction (attributed to director tumbling) and the large strain recovery observed upon removal of an applied shear stress (attributed to stored distortional elasticity). Here we are interested in the model's structural predictions.

The primary structural variable is the mesoscopic order parameter tensor, $\bar{\mathbf{S}}$, which is the traceless version of the second moment tensor of the domain distribution function:

$$\bar{\mathbf{S}} = \langle \mathbf{nn} \rangle - \frac{1}{3}\mathbf{I} \tag{1}$$

Under flow, Larson and Doi predict that the mesoscopic order parameter evolves according to

$$\frac{\mathrm{d}\bar{\mathbf{S}}}{\mathrm{d}t} = \Omega^{\mathrm{T}}\cdot\bar{\mathbf{S}} + \bar{\mathbf{S}}\cdot\Omega + \lambda\left[\frac{2}{3}\mathbf{D} + \mathbf{D}\cdot\bar{\mathbf{S}} + \bar{\mathbf{S}}\cdot\mathbf{D} - 2\bar{\mathbf{S}}:\mathbf{D}\left(\bar{\mathbf{S}} + \frac{1}{3}\mathbf{I}\right)\right] - \epsilon l\bar{\mathbf{S}} \tag{2}$$

where $\mathbf{D}$ is the rate of deformation tensor and Ω is the vorticity tensor. Most of this equation describes how director tumbling under shear influences the average domain orientation state (λ is the so-called tumbling parameter, which assumes values $|\lambda| < 1$ for tumbling nematics.) The final term on the right-hand side of eq 2 reflects the average effect of distortional elasticity. The parameter ϵ expresses the strength of distortional elastic effects (comparison with experiments suggests that this is a small number[13]), while l is a texture variable that is related to the defect density in the nematic, which obeys its own evolution equation:

$$\frac{\mathrm{d}l}{\mathrm{d}t} = II_{\mathrm{D}}l - l^2 \tag{3}$$

where II_{D} is the second invariant of $\mathbf{D}$. According to eq 3, defect density increases with increasing shear rate, so that the Larson−Doi model makes a prediction of *texture refinement*.[9] Increasing shear rate drives the texture length scale to an appropriately fine scale so that distortional elastic effects are able to balance the hydrodynamic torques, leading to a steady state.

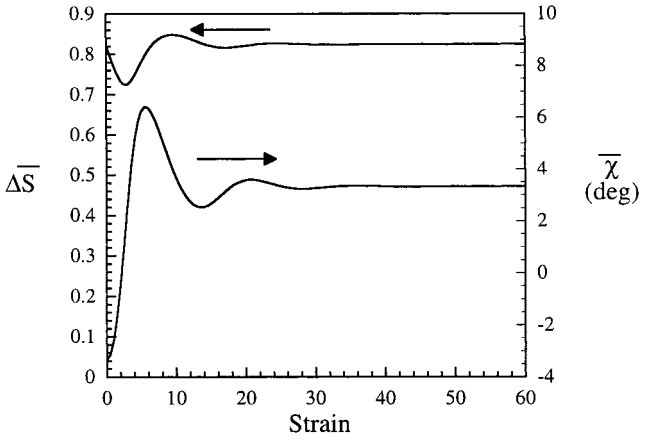

Figure 1. Larson−Doi model predictions of principal anisotropy and average orientation angle in the 1−2 plane following reversal of shear flow direction.

The three-dimensional steady-state predictions of eqs 2 and 3 in shear flow were tested extensively by Hongladarom and Burghardt; a summary may be found in ref 5. Here we focus on transient predictions, where to date only more limited tests have been possible. Hongladarom and Burghardt used flow birefringence to measure average molecular orientation in the 1−3 plane in various transient flows of PBG solutions.[7] Upon flow reversal, eq 2 predicts an initial *decrease* in orientation in the 1−3 plane, while Hongladarom and Burghardt observed an initial increase in molecular orientation. The orientation prediction for step increase in shear rate was in closer accord with experiment. Caputo and coworkers have also studied orientation in the 1−3 plane in a tumbling nematic surfactant solution using X-ray scattering and found that the surfactant solution was in closer qualitative accord with the transient orientation predictions of the Larson−Doi model than the lyotropic PBG solutions.[18] There are several quantitative discrepancies, which may result from the quadratic closure approximation used in the Larson−Doi model (see refs 18 and 19). In this paper, we emphasize the *qualitative* characteristics of this model's transient orientation predictions.

The discrepancy between prediction and experiments on PBG may be an artifact of having studied only one projection of the fluid's three-dimensional orientation state. Here we provide experimental data collected using a different projection of fluid structure. Experiments in the 1−2 plane involve measurements of both the degree of anisotropy and the average domain orientation angle (Figure 1). The former quantity is related to the principal anisotropy difference:

$$\Delta\bar{S} = \sqrt{(\bar{S}_{11} - \bar{S}_{22})^2 + 4\bar{S}_{12}^2} \tag{4}$$

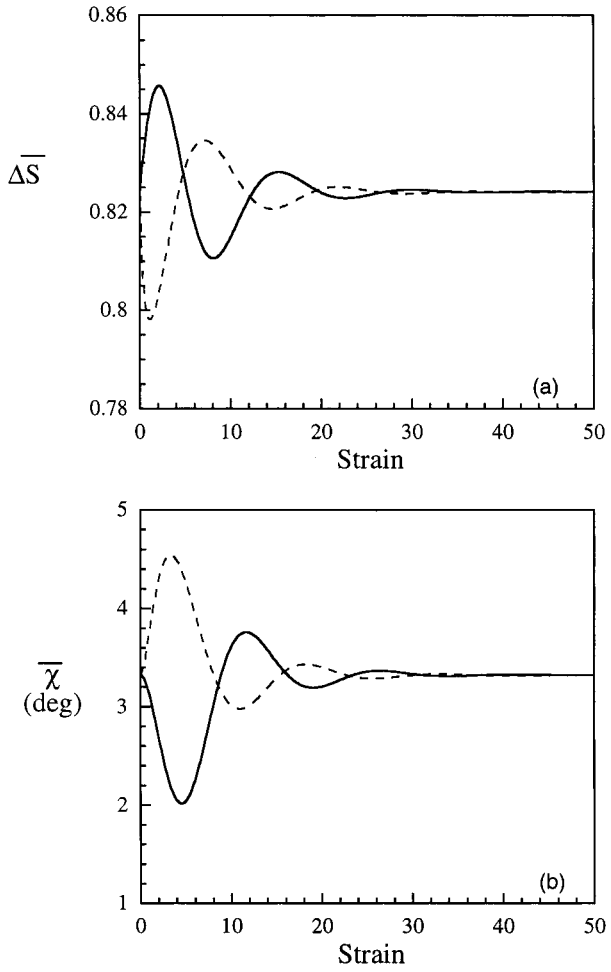

Figure 2. Larson−Doi model predictions of (a) principal anisotropy and (b) average orientation angle in the 1−2 plane following step-increase (solid curve) and step-decrease (broken curve) of shear rate by a factor of 5.

while the average domain orientation angle is given by

$$\bar{\chi} = \frac{1}{2}\tan^{-1}\left(\frac{2\bar{S}_{12}}{\bar{S}_{11} - \bar{S}_{22}}\right) \tag{5}$$

Upon flow reversal, the anisotropy is predicted to initially decrease; this qualitative behavior is common to predictions in both the 1−2 and 1−3 plane.[7] The orientation angle changes sign upon flow reversal. (In Figure 1 we adopt the convention that the final shear rate following the reversal is positive.) Starting from its prior (negative) steady-state angle, the orientation angle is predicted to exhibit a broad initial overshoot, before settling to a new steady-state value after damped oscillations.

Similar predictions for step-increase and step-decrease in shear rate are presented in Figure 2. Anisotropy and orientation angle are both predicted to exhibit damped oscillations following the transient change in flow condition. The responses for step-increase and step-decrease are almost exactly out of phase with one another. The predictions in Figures 1 and 2 were made using a "typical" parameter set, with $\epsilon = 0.03$ and with $\lambda = 0.907$ based on a dimensionless concentration $c/c^* = 1.122$ (i.e., the lowest concentration in the fully stable nematic phase).

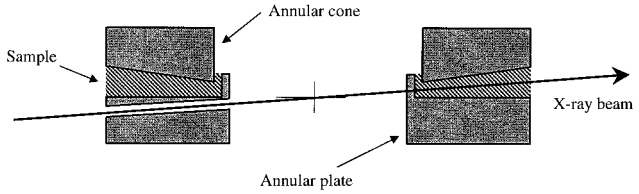

Figure 3. Schematic of annular cone and plate geometry used for X-ray measurements of fluid structure in the 1−2 plane. The cone angle has been exaggerated in this diagram; the actual cone angle is 5°.

Experimental Section

Test Fluids. Poly(γ-benzyl-L-glutamate) and poly(γ-benzyl-D-glutamate) were purchased from Sigma; the samples used in this study had reported molecular weights of 296 000 and 298 000, respectively. The polymers were combined in equal portions to create a racemic mixture, a strategy to eliminate cholestericity.[6] Hydroxypropylcellulose (Klucel E) was obtained from Aqualon; it has a nominal molecular weight of 80 000. Solvent *m*-cresol was acquired from Aldrich. The HPC was dried in a vacuum oven prior to use; other materials were used as received. Solutions were prepared gravimetrically (13.5 wt % PBG; 27 wt % HPC) and mixed over a period of 7−10 days until uniform. The PBG solution was designed to closely mimic a solution studied previously by Hongladarom and Burghardt,[8] while the HPC solution is similar to one studied earlier by Burghardt and co-workers in homogeneous shear,[20] and by Bedford and co-workers[21,22] and by Cinader and co-workers[23] in complex flows.

X-ray Shear Cell. The shear cell is based on the familiar cone and plate geometry, which provides a homogeneous shear rate throughout the device (Figure 3). However, the central portion of the cone and plate are removed, creating an annular geometry. (A similar annular device based on a parallel plate geometry was employed in a neutron shear cell developed by Noirez and Lapp,[24] and the same design concept dates farther back to a flow birefringence shear cell used by Janeschitz-Kriegl and co-workers.[25]) The cone angle in the shear cell is 5°, and the inner and outer radii of the annulus are 1.5 and 2.5 cm, respectively. The incident beam goes through a hole drilled at a 2.5° angle through the fixed lower plate, passes through the virtual tip of the cone at the center of the device, and then goes through the sample on the opposite side of the cone and plate. A thin barrier extends up from the inner edge of the lower plate to help confine the fluid in the gap between the cone and plate. However, the outer surface remains free to reduce end effects associated with parasitic velocity gradients. At high shear rates, elastic normal stresses cause the sample to be expelled from the fixture, placing an upper limit on the range of possible experiments. The path length through the sample is 1 cm, which is thick by X-ray standards. However, use of higher energy photons reduces the impact of X-ray absorption in the sample and the aluminum barrier on the inside edge of the annulus. Since the synchrotron X-ray beams used here are horizontal, the entire shear cell is mounted on a platform tilted at 2.5° to allow the beam to pass properly through the sample. Motion is provided by a microstepping motor driven by a Compumotor programmable indexer capable of delivering either oscillatory or linear motion. Provision is made for heating the fixtures, although the current experiments were carried out under ambient conditions. Full details on the shear cell design will be presented in a forthcoming publication.

Experimental Methods. Experiments were performed on beamline 5BM-D of the Advanced Photon Source at Argonne National Lab. Unfocused bending magnet radiation with an energy of 25 keV (wavelength = 0.50 Å) was directed at the hole drilled through the lower plate, which defined the beam passing through the sample (diameter = 1 mm). A vacuum chamber was placed between the shear cell and the detector to reduce background air scattering. Two-dimensional digital X-ray scattering patterns were collected on a CCD detector

(MarCCD) and stored for subsequent analysis. When collecting steady-state images, or prior to initiating a transient change in shear flow condition, the sample was presheared for at least 150 strain units.

Data Analysis Procedures. The X-ray scattering patterns exhibited the anisotropy typical of sheared nematic polymers (Figure 4). Scattering from the PBG solution took the form of a "bow tie" pattern oriented roughly perpendicular to the flow direction (Figure 4a,b), indicating alignment of the rodlike molecules generally along the flow direction. At this modest concentration there is only weak correlation in the lateral packing of the rodlike molecules and hence no strong correlation peak in the structure factor. Instead, this type of pattern may be thought of as a convolution of the highly anisotropic form factor for a single rod with the overall distribution of molecular orientation[26] (bearing in mind that this reflects both the local distribution of molecular orientation around the director and the distribution of director orientation in the polydomain sample). In the HPC solution, the higher concentration leads to a stronger correlation in the positions of neighboring molecules, and there is a well-defined peak in scattering intensity as a function of scattering vector, q (Figure 4c).

Quantitative measures of molecular orientation were extracted from azimuthal scans of intensity. A wide q range was used in computing azimuthal scans to maximize the intensity available for transient measurements with short exposure times. The angular range used for PBG and HPC solutions is superimposed on the images in Figure 4a,c. Figure 5 presents typical azimuthal intensity scans for PBG sheared at steady state in two directions, extracted from the images in Figure 4a,b. The two scans nearly superimpose, indicating that the average domain orientation angle is very close to the flow direction under these conditions. (In fact, analysis of these scans shows that the steady-state orientation angle is around 0.5°.) Prior to subsequent analyses, the azimuthal scans are normalized, and a common baseline value is subtracted from all scans measured for a given sample. The baseline value is taken to be the lowest intensity measured in any azimuthal scan and typicaly corresponds to a pattern with a high degree of molecular orientation in which little scattering is expected to occur along the flow direction.

Anisotropic X-ray scattering patterns are often analyzed to determine an orientation parameter. However, standard methods of analysis assume a uniaxial distribution of orientation about a predetermined symmetry axis, conditions that are not generally met in shear flow. Here we instead use a simple method to directly characterize anisotropy in the X-ray scattering pattern.[27] A point on the azimuthal scan is represented by a unit vector, **u**. Anisotropy in the X-ray scattering pattern is then characterized by computing the second moment tensor,

$$\langle \mathbf{uu} \rangle = \begin{bmatrix} \langle u_1 u_1 \rangle & \langle u_1 u_2 \rangle \\ \langle u_1 u_2 \rangle & \langle u_2 u_2 \rangle \end{bmatrix} = \begin{bmatrix} \langle \cos^2 \beta \rangle & \langle \sin \beta \cos \beta \rangle \\ \langle \sin \beta \cos \beta \rangle & \langle \sin^2 \beta \rangle \end{bmatrix} \quad (6)$$

where $\langle \cdots \rangle$ represents an average weighted by the azimuthal intensity distribution $I(\beta)$, where β is measured from the flow direction (see Figure 4). For instance, the 11-component is given by

$$\langle \cos^2 \beta \rangle = \frac{\int_0^{2\pi} \cos^2 \beta I(\beta)\, \mathrm{d}\beta}{\int_0^{2\pi} I(\beta)\, \mathrm{d}\beta} \quad (7)$$

We report an "anisotropy factor", taken to be the difference in the principal values of the second moment tensor, $[(\langle u_1 u_1 \rangle - \langle u_2 u_2 \rangle)^2 + 4\langle u_1 u_2 \rangle^2]^{1/2}$, while the average orientation direction is computed from the principal directions of the second moment tensor. Noting that scattering from rodlike molecules is concentrated perpendicular to their axes, the average orientation direction is given by the eigenvector associated with the smaller of the two principal values.[27]

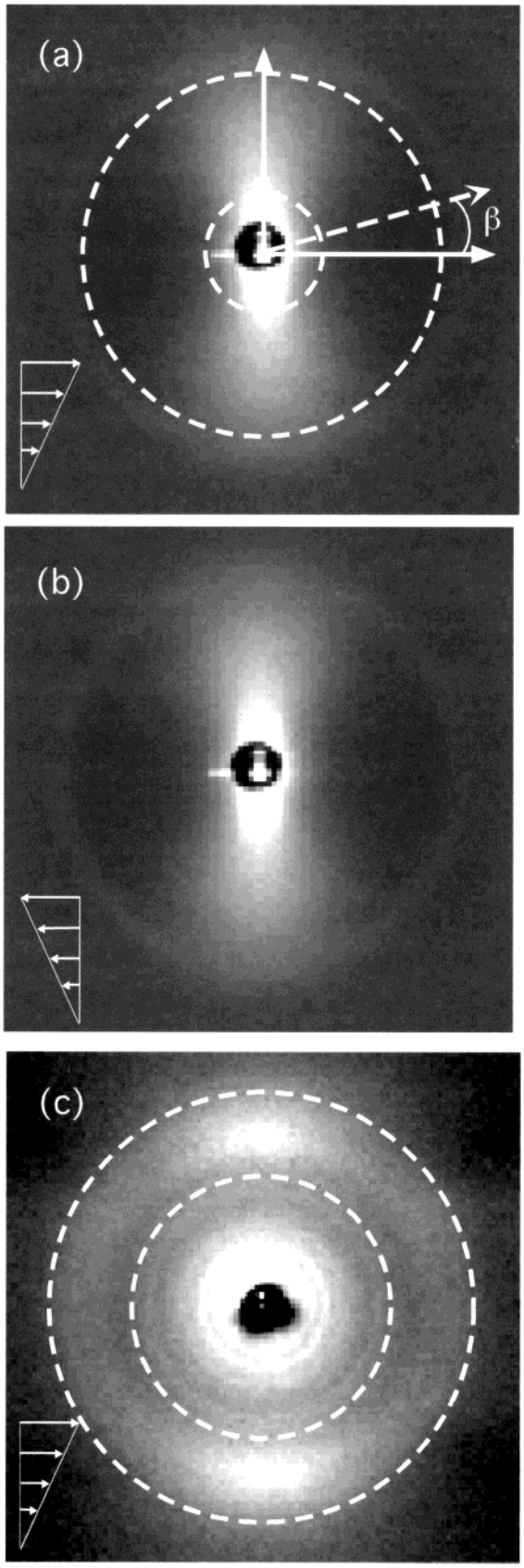

Figure 4. Representative scattering patterns: (a) PBG, 0.2 s^{-1}, forward direction; (b) PBG, 0.2 s^{-1}, reverse direction; (c) HPC, 4.0 s^{-1}.

Any small misalignment of the shear cell relative to the pixel array in the detector will lead to systematic errors in the measured orientation angle. To compensate for this, several

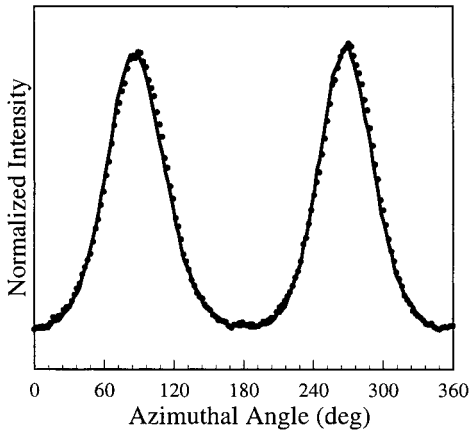

Figure 5. Azimuthal intensity scans extracted from 2-D scattering patterns collected for PBG at 1.0 s^{-1} in the forward (−) and reverse (●) directions.

experiments were conducted in both the forward and reverse directions (as in Figure 4a,b), and a single orientation angle correction factor was extracted by comparing pairs of raw angles computed directly from the patterns. Separate factors were determined for the PBG and HPC data, since these experiments were performed on two separate occasions.

Results and Discussion

Steady Orientation Behavior. Measurements of orientation of the PBG solution in the 1−2 plane follow previously established behavior[5] (Figure 6). The anisotropy factor exhibits a low shear rate plateau, followed by a transition to a higher orientation state at higher shear rates (Figure 6a). It has been established that this reflects a transition from tumbling at low shear rates to flow aligning dynamics at high shear rates as predicted by the Doi model.[28] The orientation angle is small and positive at low rates and then changes sign to become negative at intermediate rates (Figure 6b). Orientation angle data collected by Hongladarom and Burghardt on a similar PBG solution using an angled birefringence technique[8] are reproduced in Figure 6b and agree very favorably with the measurements presented here. These results demonstrate that small changes in orientation angle may be accurately followed using the X-ray scattering method. The Doi model predicts two sign changes in average orientation angle as a function of shear rate, closely correlated with sign changes in the first and second normal stress difference.[5,28] The X-ray data clearly show the predicted first sign change; unfortunately, X-ray experiments could not be pursued to high rates owing to expulsion of the test fluid from the shear cell. However, the previously collected birefringence data also show a trend toward a second sign change at high rates.

Figure 6a also presents data extracted from earlier X-ray measurements conducted on a similar PBG solution using a rotating disk shear cell that probes molecular orientation in the 1−3 plane.[11] To make this comparison, the original raw X-ray patterns were subjected to a data analysis procedure identical to that described above for the 1−2 plane measurements. In particular, it was necessary to extract new azimuthal scans from the old images using the same range of scattering angle as depicted in Figure 4a. Using the same measure of anisotropy in the X-ray scattering patterns, it is clear that there is a higher degree of molecular orientation in the low shear rate regime when

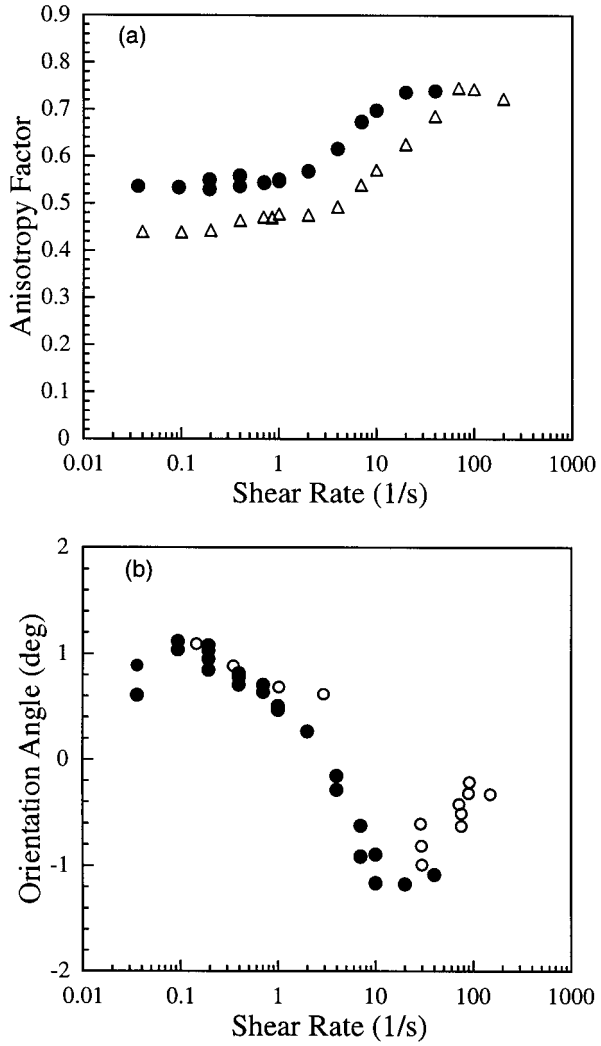

Figure 6. Steady-state molecular orientation in 13.5 wt % PBG in *m*-cresol. (a) Anisotropy factor as a function of shear rate: (●) 1−2 plane measurements; (△) 1−3 plane measurements (reanalyzed data from ref 11). (b) Average orientation angle as a function of shear rate: (●) 1−2 plane X-ray measurements; (○) results of prior angled birefringence measurements on a similar PBG solution.[8]

the sheared LCP is viewed from "the side" (i.e., 1−2 plane measurements) rather than from "above" (i.e., 1−3 plane measurements). Thus, the overall orientation state does not possess uniaxial symmetry but rather is biaxial. The same conclusion was reached by Hongladarom and Burghardt, who extracted a measure of transverse anisotropy from their angled birefringence technique.[8] Both experiments indicate that there is a higher probability of finding molecules pointing along the 3-direction than along the 2-direction at low shear rates, in qualitative agreement with the steady state prediction of the Larson−Doi model.[5] At higher shear rates, these differences become less pronounced, so that the overall orientation state is more closely uniaxial.

Steady data collected for the HPC solution show some similarities in behavior, but also some noteworthy differences (Figure 7). In this case, as well, we have reanalyzed previous X-ray data collected in the 1−3 plane on a similar HPC solution[11] to allow direct comparison to the present measurements. Our earlier optical and X-ray studies of 27 wt % HPC in *m*-cresol in the 1−3 plane showed indications of two transitions

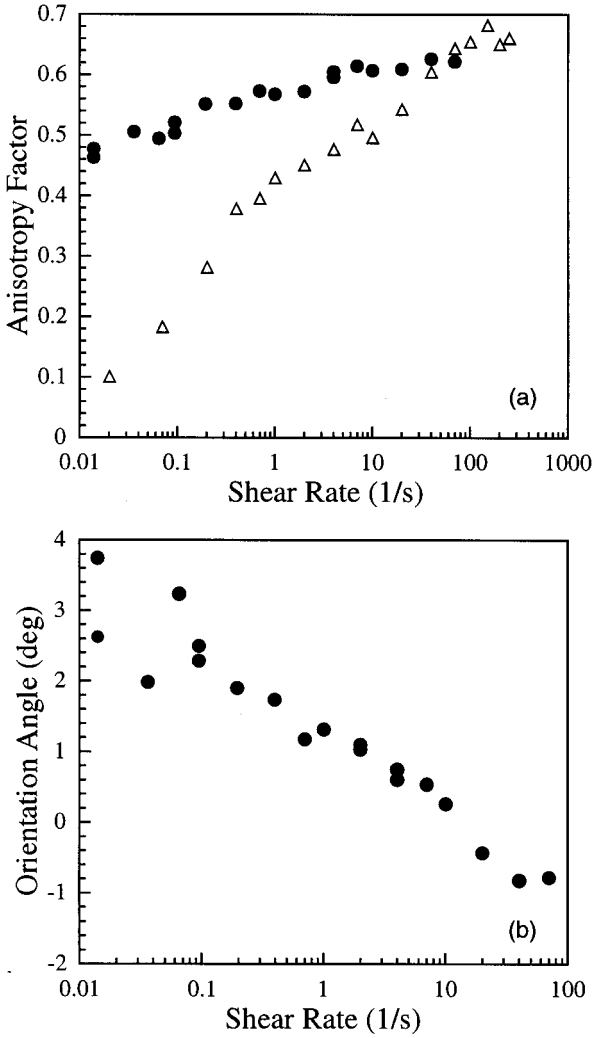

Figure 7. Steady-state molecular orientation in 27 wt % HPC in *m*-cresol. (a) Anisotropy factor as a function of shear rate: (●) 1−2 plane measurements; (△) 1−3 plane measurements (reanalyzed data from ref 11). (b) Average orientation angle as a function of shear rate.

in orientation: first from low orientation at low rates to moderate orientation at intermediate rates and then a second transition to still higher molecular orientation at high shear rates.[11,20] The second region of increasing orientation corresponds well to independent measurements of sign changes in the first normal stress difference, indicating that it is associated with the transition from tumbling to flow aligning dynamics, similar to the transition seen in PBG above. The origin of the low orientation at the lowest rates is less clear, although we have speculated that it might reflect a persistent cholesteric phase.[20] By comparison, the current measurements of anisotropy in the 1−2 plane are rather plain, showing only a general increasing trend in orientation with shear rate. Most remarkable is the large difference in anisotropy measured in the 1−2 and 1−3 planes in the limit of low rates. While the sample becomes nearly isotropic when viewed along the velocity gradient direction, there is still significant anisotropy when viewed from the side along the vorticity direction.

The strong anisotropy in molecular orientation state in the transverse direction in the HPC solution provides a direct explanation for a previously puzzling result. Bedford and Burghardt studied molecular orientation in pressure-driven slit flow of a similar HPC solution.[21] Their measurements employed a light beam directed along the dominant shear gradient and hence probed molecular orientation in the 1−3 plane. Near the edges of the slit flow, they observed large increases in birefringence, whose magnitude could not be easily explained. In this region, parasitic velocity gradients associated with the no-slip condition on the side wall of the slit flow cell mean that the light beam actually passes along the vorticity direction of the local shearing deformation and hence locally probes anisotropy in the 1−2 shear plane. As seen in Figure 7a, there is much stronger molecular orientation in HPC at low rates when viewed from this perspective, explaining the observation of Bedford and Burghardt.[21]

Why is such a large difference in molecular orientation observed in the HPC solution, depending on the direction in which anisotropy is measured? One possible explanation relates to the hypothesis that the low orientation observed in the 1−3 plane in HPC solutions is due to the persistence of a cholesteric phase at low shear rates. If one envisions a cholesteric phase in which the axis of the cholesteric helix is aligned along the shear gradient (2) direction, then one naturally predicts zero anisotropy in the 1−3 plane while still maintaining significant anisotropy in the 1−2 plane. This interpretation is somewhat bolstered by the appearance of vivid Bragg interference colors from more highly concentrated HPC solutions sheared at low rates that are consistent with the axis of the cholesteric helix pointed along the velocity gradient.[29]

The steady orientation angle in the HPC solution exhibits grossly similar features to that measured in PBG; it is positive at low rates and becomes negative at higher rates. (Again, experiments could not be extended to higher rates owing to expulsion of the sample from the shear cell.) Together with data reported above for PBG solutions, and an additional set of angled-light birefringence data measured on an aqueous HPC solution,[10] these data provide a third case in which the orientation angle in a sheared lyotrope passes from positive to negative values in the shear rate range where the first normal stress difference changes sign, in agreement with predictions of the Doi molecular model and confirming the molecular explanation for negative normal stresses originally advanced by Maffettone and Marrucci.[30]

Transient Orientation Behavior: Relaxation. Upon cessation of shear flow at low rates, the PBG solution exhibits an increase in the degree of orientation measured in the 1−2 plane (Figure 8a). These data are consistent with both prior optical[7] and X-ray[11] data collected in the 1−3 plane on similar moderately concentrated PBG solutions. Consistent with other relaxation processes in PBG solutions,[31,32] the transient orientation change is seen to occur on a time scale that varies inversely with previously applied shear rate, so that the data nearly superimpose when plotted as a function of time scaled by the prior shear rate. Accompanying this increase in degree of orientation is a simultaneous change in the average domain orientation *direction* (Figure 8b). At these low rates, the steady-state orientation angle is small and positive; upon flow cessation, the orientation angle changes sign and becomes negative. Indeed, the magnitude of the negative orientation angle measured long after flow cessation is larger than observed during shear at any rate. Using

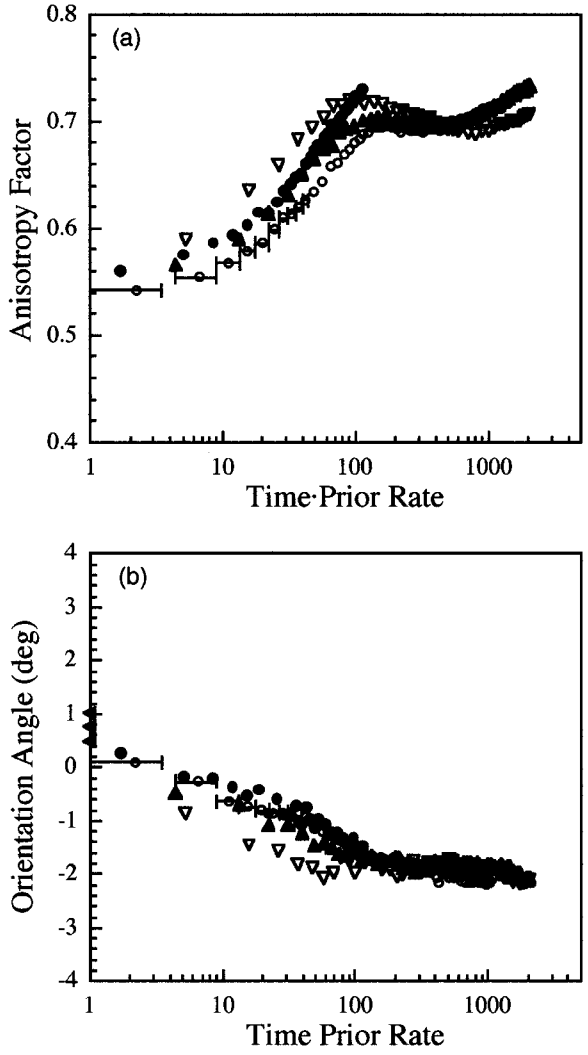

Figure 8. Relaxation upon cessation of shear flow in 13.5 wt % PBG in *m*-cresol. Prior shear rates are 0.2 s^{-1} (○, ●; repeated experiment), 0.5 s^{-1} (▲), and 1.0 s^{-1} (▼). Representative horizontal error bars indicate the time period over which each scattering pattern is acquired. (a) Anisotropy factor as a function of scaled time. (b) Average orientation angle as a function of scaled time. Triangles on left axis indicate prior steady-state orientation angles at the three shear rates.

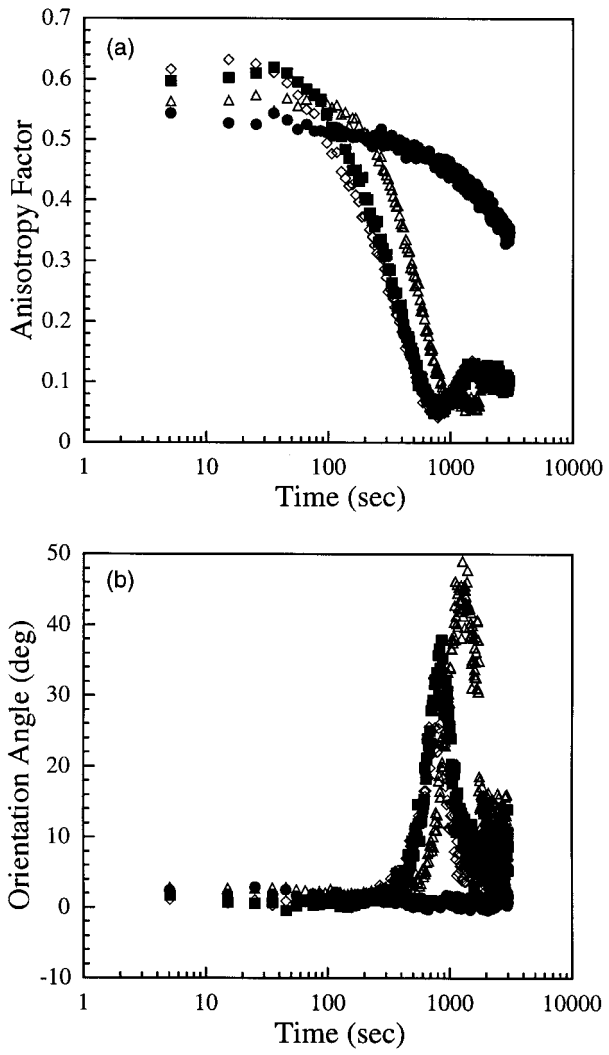

Figure 9. Relaxation upon cessation of shear flow in 27 wt % HPC in *m*-cresol. Prior shear rates are 0.1 s^{-1} (●), 0.4 s^{-1} (△), 1.0 s^{-1} (■), and 2.0 s^{-1} (◇). (a) Anisotropy factor as a function of time. (b) Average orientation angle as a function of time.

their angled light birefringence technique, Hongladarom and Burghardt inferred that such a sign change must take place, since they could measure the positive steady-state angle and the negative angle achieved at long times.[8] However, this method lacked the time resolution to follow the transient evolution.

Moldenaers and co-workers used transient stress measurements in intermittent flow experiments to probe time-dependent changes in PBG fluid structure during relaxation.[33] They observed phase shifts in the location of stress maxima and minima observed following resumption of shear (or reversal of shear) which depended on the length of time the sample had relaxed. Changes in average domain orientation angle during relaxation documented here in Figure 8b provide an appealing explanation for phase shifts in subsequent stress oscillations upon flow resumption. However, the details of the transient stress behavior observed by Moldenaers et al. are too complex to ascribe to a single simple mechanism; it is likely that simultaneous consideration of evolution in both the direction and degree of average domain orientation would be necessary to unravel the types of transient behavior documented in this earlier work.[33]

The relaxation behavior of HPC is markedly different than that observed in PBG (Figure 9). In all cases, the orientation is observed to decay upon flow cessation (Figure 9a). This gross difference in orientation behavior upon relaxation is believed to explain a similar difference in evolution of dynamic modulus upon flow cessation: moduli are observed to decrease in PBG[34] and increase in HPC.[35] At low shear rates, the decay is sluggish, but it becomes more rapid at somewhat higher shear rates. Note, however, that at the two highest rates presented in Figure 9 the relaxation occurs over nearly identical time scales; the prior shear rate appears not to influence the relaxation rate in this regime, in contrast to the scaling noted above for PBG. The general trends in molecular orientation observed here closely parallel those found by Burghardt and co-workers in 1−3 plane birefringence studies of relaxation in a similar HPC/cresol solution, including the small "rebound" in anisotropy observed at longer times,[20] and, further, are similar to previous measurements in aqueous HPC.[10] The orientation angle data are quite dra-

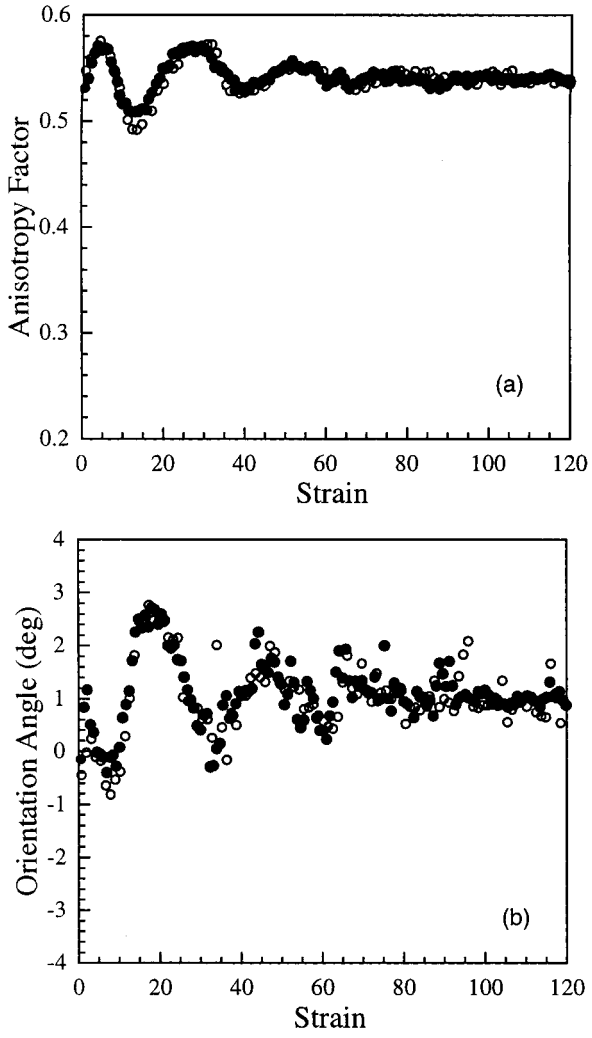

Figure 10. Shear flow reversal in 13.5 wt % PBG in *m*-cresol, at rates of 0.04 s^{-1} (●) and 0.1 s^{-1} (○). (a) Anisotropy factor as a function of shear strain following the reversal. (b) Average orientation angle as a function of shear strain following the reversal.

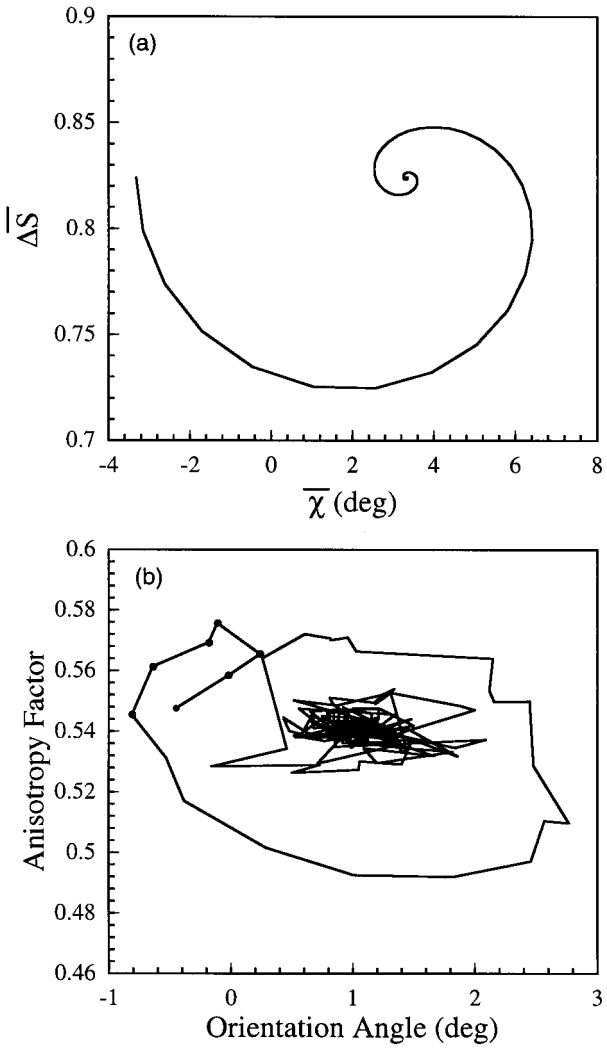

Figure 11. Alignment trajectories in reversal (a) Larson−Doi computation and (b) experiment. In (b), data points during the first nine strain units are denoted with symbols.

matic (Figure 9b); however, the large variations seen here are likely consequences of the fact that accurate determination of orientation angles becomes increasingly difficult as the pattern becomes more isotropic. Indeed, the orientation angle is undefined for an isotropic pattern. It is likely that some weak anisotropy in the background scattering comes to dominate the measurement when the scattering from the LCP solution becomes nearly isotropic. Comparison of parts a and b of Figure 9 shows that the measured orientation angle reaches its most extreme excursions at the point where the measured anisotropy is weakest.

Transient Orientation Behavior: Reversals. In agreement with previous birefringence experiments in the 1−3 plane,[7] these 1−2 plane X-ray scattering measurements confirm that the average molecular orientation of this PBG solution initially increases upon reversal of shear flow direction (Figure 10a). Comparison with Figure 1 shows that the discrepancy between experiment and the prediction of the Larson−Doi model remains and was not an artifact of either the birefringence technique employed by Hongladarom and Burghardt[7] or the restriction to the 1−3 plane in previous transient measurements of LCP orientation. In addition to the disagreement in the average degree of orientation, the average orientation direction similarly exhibits unusual behavior immediately following the reversal (Figure 10b). While the Larson−Doi model predicts a smooth, large initial overshoot as the angle initially changes signs, the data show an abrupt increase and decrease in orientation angle, followed by a more gradual, large overshoot.

It is interesting to note that both the anisotropy and orientation angle data would be in much closer qualitative agreement with Larson−Doi model predictions if, somehow, data obtained during the first 10 or so strain units could be ignored. This point is made clearly by examining "orientation trajectories" comprised of a cross plot of anisotropy vs orientation angle (Figure 11). This representation is similar to cross plots used by Moldenaers and co-workers to characterize transient rheology in the tumbling regime.[36] The Larson−Doi model predicts a smooth counterclockwise spiral from the prior steady state with negative orientation angle toward the new steady state with positive orientation angle (Figure 11a; again, notice the initial decrease in predicted anisotropy). The experimental data instead show that both anisotropy and angle make a temporary initial increase, then return to near their starting points, and finally continue on a trajectory that agrees quite satisfactorily with the qualitative characteristics of the

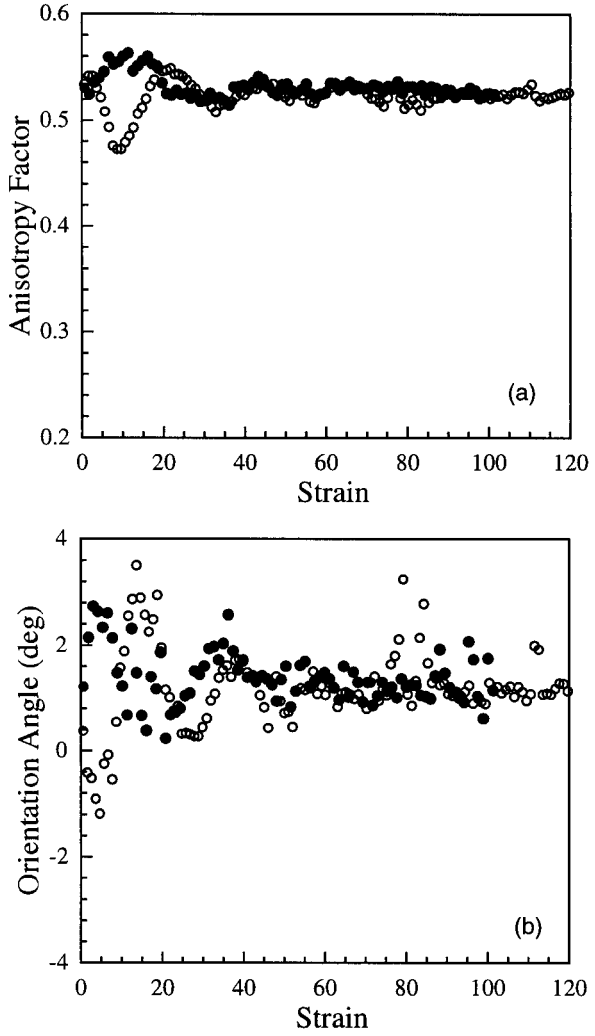

Figure 12. Step changes in shear rate in 13.5 wt % PBG in *m*-cresol. Step-increase from 0.02 to 0.1 s^{-1} (●). Step-decrease from 0.2 to 0.04 s^{-1} (○). (a) Anisotropy factor as a function of shear strain following the step change. (b) Average orientation angle as a function of shear strain following the step change.

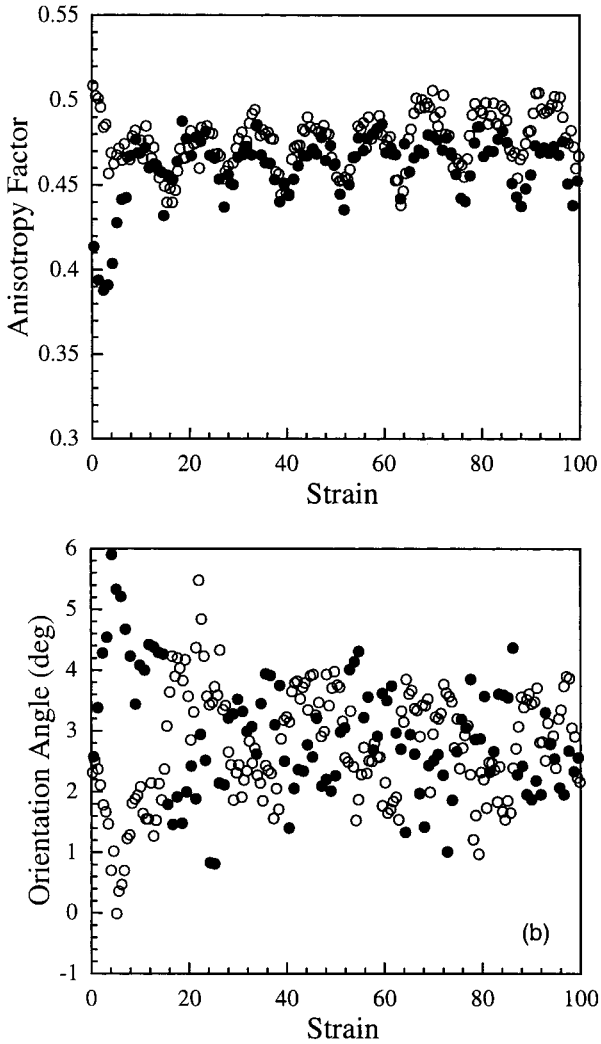

Figure 13. Step changes in shear rate in 27 wt % HPC in *m*-cresol. Step-increase from 0.02 to 0.1 s^{-1} (●). Step-decrease from 0.2 to 0.04 s^{-1} (○). (a) Anisotropy factor as a function of shear strain following the step change. (b) Average orientation angle as a function of shear strain following the step change.

Larson−Doi model prediction. (In Figure 11, data collected during the first nine strain units following the reversal are highlighted with symbols.) In fact, a careful examination of mechanical data collected following shear flow reversal[36] shows an initial transient that does not agree with the details of Larson−Doi predictions.[13] As discussed by Vermant and co-workers,[37] the clearest discrepancy is in transient first normal stress difference data, which show an initial decrease over the first seven strain units or so for a number of LCPs, in contrast to Larson−Doi predictions of an abrupt drop in N_1 upon reversal, followed by an increase with applied strain. As in Figure 11, this discrepancy may be visualized by comparing the stress trajectories of Moldenaers and coworkers[36] with a trajectory computed using the model.[38]

Since the discrepancy involves behavior shortly after the reversal, it is tempting to attribute it to molecular viscoelastic effects that are ignored within the Larson−Doi theory. However, we do not feel that molecular effects provide a satisfactory explanation. The experiments in question here are collected at shear rates nearly 2 orders of magnitude lower than where molecular viscoelastic effects come into play in driving the tumbling−aligning transition. Put another way, this initial period of around 10 strain units plays out over 100 s at a rate of 0.1 s^{-1} and even longer at the lower rate used in Figure 10. This is much longer than a reasonable estimate of molecular relaxation time of around 0.1 s in typical PBG solutions. Finally, we point out that these "short" time anisotropy and orientation angle data both scale quite well with shear strain when the reversal experiment is repeated at a different rate (Figure 10), which, in LCPs, is typically a good indicator that the Deborah number is small.

Transient Orientation Behavior: Step Changes. Measurements of the average degree of molecular orientation in the 1−2 plane following step-increase and step-decrease in shear rate agree more favorably with the Larson−Doi model (Figure 12a). In particular, step-increase in rate leads to an initial increase in orientation, while step-decrease in rate has the opposite effect, in good qualitative agreement with the model predictions (Figure 2a). Despite the model's somewhat better performance in step-change experiments, measurements of average orientation angle reveal, again, a serious discrepancy (Figure 12b). Note that the data show an initial increase in orientation angle upon a step-increase in shear rate and an initial decrease in orientation angle upon a step-decrease in shear rate. This is exactly

opposite to the predictions of the Larson−Doi model (Figure 2b).

Results from similar experiments on HPC are presented in Figure 13. These data are characterized by considerably greater noise in the measurements of orientation angle and a suspicious periodic oscillation in anisotropy factor. In fact, the oscillation period is equal to precisely one-sixth of the rotation period of the cone (1 rotation = 72 strain units). Such a period is difficult to rationalize. The rotating cone is supported by three ceramic posts. Thus, any errors due to misalignment of the cone and plate might be expected to have a period of one or $^1/_3$ of a revolution rather than $^1/_6$ of a revolution. Instead, the most likely explanation appears to be that stray air scattering from the X-ray beam incident on the shear cell causes each of the three support posts to cast a weak shadow on the face of the detector every time it passes above the beam, which happens *twice* for each period of rotation of the cone. This would lead to a time-dependent and anisotropic contribution to the background scattering that would contribute to the overall anisotropy factor computed from the scattering pattern. Steady-state data, collected using much longer exposure times, should be more reliable, as should also the relaxation data, in which the cone is not rotating. Apparently, the details of the experimental setup used for the PBG experiments avoided this defect. Despite the poor quality of the data in Figure 13, it is worth noting that the initial response in orientation angle (Figure 13b) closely resembles that seen in PBG (Figure 12b), again precisely opposite the orientation angle predictions of the Larson−Doi model (Figure 2b).

Summary

We have described an annular cone and plate X-ray shear cell that allows for real time measurement of complex fluid structure in the 1−2 plane. This has allowed the first transient measurements of both the average degree and average direction of molecular orientation in sheared liquid crystalline polymer solutions. Coordination of 1−2 and 1−3 plane measurements in a PBG and an HPC solution reveals that the average orientation state is not uniaxially symmetric at low rates. In both cases, there is an enhancement in the probability of finding molecules oriented along the 3-direction relative to the 2-direction, a fact that is quite dramatic in the case of HPC at low rates. Both LCPs show a sign change in the average orientation angle from positive to negative values with increasing shear rate that is correlated with the change in sign of the first normal stress difference. Upon cessation of shear flow, PBG exhibits an increase in molecular orientation, while HPC shows a loss of orientation.

In transient flow protocols, these data provide an opportunity for more stringent and precise tests of the orientation state predictions of the Larson−Doi polydomain model than have been possible to date. In shear flow reversal, data collected on PBG confirm that the degree of molecular orientation initially increases upon reversal of the flow direction, a response that is coordinated with a temporary increase in the orientation angle. Neither of these observations agree with Larson−Doi model predictions, but the response after an initial period of around 10 strain units following the reversal comes into excellent qualitative agreement with the model predictions. Similar short-time discrepancies in mechanical behavior have been previously described.[37] Upon step-increase or -decrease in shear rate, the Larson−Doi model performs better in predicting the qualitative response of the degree of molecular orientation but predicts exactly the wrong trends for the average orientation angle.

The root causes for the discrepancies between the Larson−Doi model and the experiment are not clear. However, since the experiments in question were collected at rather low shear rates, it does not appear likely that molecular-level phenomena are responsible. Measurements of transient molecular orientation in the 1−3 plane in tumbling nematic surfactant solutions have shown better agreement with the Larson−Doi predictions;[18] it would be interesting to study such surfactant samples using the current methods to further explore the applicability of this model to nonpolymeric nematic fluids.

Acknowledgment. We acknowledge financial support from the donors of the Petroleum Research Fund of the American Chemical Society. X-ray experiments were conducted at the DuPont-Northwestern-Dow Collaborative Access Team (DND-CAT) Synchrotron Research Center located at Sector 5 of the Advanced Photon Source. DND-CAT is supported by the E.I. DuPont de Nemours & Co., the Dow Chemical Company, and the National Science Foundation through Grant DMR-9304725 and the State of Illinois through the Department of Commerce and the Board of Higher Education Grant IBHE HECA NWU 96. Use of the Advanced Photon Source was supported by the U.S. Department of Energy, Basic Energy Sciences, Office of Energy Research, under Contract W-31-102-Eng-38.

References and Notes

(1) Fuller, G. G. *Optical Rheometry of Complex Fluids*; Oxford: New York, 1995.
(2) Larson, R. G. *The Structure and Rheology of Complex Fluids*; Oxford: New York, 1999.
(3) Srinivasarao, M.; Berry, G. C. *J. Rheol.* **1991**, *35*, 379.
(4) Burghardt, W. R.; Fuller, G. G. *Macromolecules* **1991**, *24*, 2546.
(5) Burghardt, W. R. *Macromol. Chem. Phys.* **1998**, *199*, 471.
(6) Hongladarom, K.; Burghardt, W. R.; Baek, S. G.; Cementwala, S.; Magda, J. J. *Macromolecules* **1993**, *26*, 772.
(7) Hongladarom, K.; Burghardt, W. R. *Macromolecules* **1993**, *26*, 785.
(8) Hongladarom, K.; Burghardt, W. R. *Macromolecules* **1994**, *27*, 483.
(9) Burghardt, W. R.; Hongladarom, K. *Macromolecules* **1994**, *27*, 2327.
(10) Hongladarom, K.; Secakusuma, V.; Burghardt, W. R. *J. Rheol.* **1994**, *38*, 1505.
(11) Hongladarom, K.; Ugaz, V. M.; Cinader, D. K.; Burghardt, W. R.; Quintana, J. P.; Hsiao, B. S.; Dadmun, M. D.; Hamilton, W. A.; Butler, P. D. *Macromolecules* **1996**, *29*, 5346.
(12) Ugaz, V. M.; Cinader, D. K., Jr.; Burghardt, W. R. *Macromolecules* **1997**, *30*, 1527.
(13) Larson, R. G.; Doi, M. *J. Rheol.* **1991**, *35*, 539.
(14) Leslie, F. M. *Adv. Liq. Cryst.* **1979**, *4*, 1.
(15) Hess, S. *Z. Naturforsch.* **1976**, *31A*, 1034.
(16) Doi, M. *J. Polym. Sci., Polym. Phys. Ed.* **1981**, *19*, 229.
(17) Kuzuu, N.; Doi, M. *J. Phys. Soc. Jpn.* **1984**, *53*, 1031.
(18) Caputo, F. E.; Burghardt, W. R.; Berret, J. F. *J. Rheol.* **1999**, *43*, 765.
(19) Kawaguchi, M. N.; Denn, M. M. *J. Rheol.* **1999**, *43*, 111.
(20) Burghardt, W.; Bedford, B.; Hongladarom, K.; Mahoney, M. In *Flow-Induced Structure in Polymers*; Nakatani, A. I.,

Dadmun, M. D., Eds.; ACS Symposium Series 597; American Chemical Society: Washington, DC, 1995; p 308.
(21) Bedford, B. D.; Burghardt, W. R. *J. Rheol.* **1996**, *40*, 235.
(22) Bedford, B. D.; Cinader, D. K., Jr.; Burghardt, W. R. *Rheol. Acta* **1997**, *36*, 384.
(23) Cinader, D. K., Jr.; Burghardt, W. R. *Polymer* **1999**, *40*, 4169.
(24) Noirez, L.; Lapp, A. *Phys. Rev. Lett.* **1997**, *78*, 70.
(25) Janeschitz-Kriegl, H. *Polymer Melt Rheology and Flow Birefringence*; Springer: Berlin, 1983.
(26) Walker, L. M.; Wagner, N. J. *Macromolecules* **1994**, *27*, 5979.
(27) Cinader, D. K., Jr.; Burghardt, W. R. *J. Polym. Sci., Part B: Polym. Phys.* **1999**, *37*, 3411.
(28) Larson, R. G. *Macromolecules* **1990**, *23*, 3983.
(29) Hongladarom, K.; Burghardt, W. R. *Rheol. Acta* **1998**, *37*, 46.
(30) Marrucci, G.; Maffettone, P. L. *Macromolecules* **1989**, *22*, 4076.
(31) Moldenaers, P.; Mewis, J. *J. Non-Newtonian. Fluid Mech.* **1990**, *34*, 359.
(32) Larson, R. G.; Mead, D. W. *J. Rheol.* **1989**, *33*, 1251.
(33) Moldenaers, P.; Yanase, H.; Mewis, J. *J. Rheol.* **1991**, *34*, 1681.
(34) Moldenaers, P.; Mewis, J. *J. Rheol.* **1986**, *30*, 567.
(35) Grizzuti, N.; Moldenaers, P.; Mortier, M.; Mewis, J. *Rheol. Acta* **1993**, *32*, 218.
(36) Moldenaers, P.; Mortier, M.; Mewis, J. *Chem. Eng. Sci.* **1994**, *49*, 699.
(37) Vermant, J.; Mortier, M.; Moldenaers, P.; Mewis, J. *Rheol. Acta* **1999**, *38*, 537.
(38) Larson, R. G. *Rheol. Acta* **1996**, *35*, 150.

MA0107556